Published in final edited form as:
Stem Cells Dev. 2006 August ; 15(4): 595–608. doi:10.1089/scd.2006.15.595.

DENTAL FOLLICLE PROGENITOR CELL HETEROGENEITY IN THE DEVELOPING MOUSE PERIODONTIUM

Xianghong Luan, **Yoshihiro Ito**, **Smit Dangaria**, and **Thomas G.H. Diekwisch**
Brodie Laboratory for Craniofacial Genetics, The University of Illinois at Chicago, College of Dentistry, Departments of Orthodontics and Oral Biology

Abstract

As a developmental precursor for diverse periodontal tissues the dental follicle harbors great promise for periodontal tissue regeneration. However, development of optimal therapy awaits the answer to a key question that impinges on many issues in development; do adult progenitor tissues form a homogeneous cell population that differentiates into target tissues when they arrive at the site, or they contain heterogeneous cell populations that are committed to specific fates? In order to address the homogeneity/heterogeneity question we analyzed differentiation pathways and markers in several cloned dental follicle cell lines. Our studies revealed that each of our cloned dental follicle lines featured remarkably unique characteristics indicative of a separate and distinct lineage. One line, DF1 was high in proliferative activity while it did not display any mineralization behavior, suggesting that it might be related to a periodontal ligament-type lineage. DF2 was similar to DF1 but featured remarkably high alkaline phosphatase activity indicative of a highly undifferentiated state. DF3 matched the mineralization characteristics of a same stage alveolar bone line AB1 in terms of gene expression and von Kossa staining indicating that DF3 might be of cementoblastic or alveolar bone osteoblastic lineage. In order to verify the multilineage potential of the dental follicle for purposes of tissue engineering, a series of differentiation induction experiments was conducted. For identification purposes, characteristics of these heterogeneous follicular progenitor cells were compared with follicle components in tissue sections of the postnatal developing periodontium. The presence of heterogeneous cell populations in the dental follicle mirrors individual developmental pathways in the formation of the dental integument. The profound cellular heterogeneity of the dental follicle as an adult progenitor for tissue regeneration also suggests that heterogeneous cellular constituents might play as much of a role in tissue regeneration as the inducible characteristics of individual lineages might do.

Introduction

The cellular basis of tissue regeneration builds both on the abilities of progenitor cells to transdifferentiate into various lineages and/or on the multipotent capabilities of stem cells to differentiate into desired target tissues. These pluripotent and multipotent cells reside within the body in various blastemas and connective tissues and are not limited to embryonic tissues (1). Specifically, it has been demonstrated that two general categories of reserve precursor cells exist within the body and are involved in the maintenance and repair of tissues in adults: lineage-committed progenitor cells and lineage-uncommitted pluripotent stem cells (1). As a consequence, it is often not clear whether the differentiation capability of a multipotent adult

Author for Correspondence: Thomas G.H. Diekwisch, D.M.D., Ph.D. (sc.), Ph.D. (phil.) Professor and Head, Department of Oral Biology, Director, Brodie Laboratory for Craniofacial Genetics, Allan G. Brodie Endowed Chair for Orthodontic Research, Professor of Anatomy/Cell Biology, Bioengineering, Orthodontics, Periodontics, UIC College of Dentistry, 801 South Paulina Street, MC 690, Chicago, Illinois 60612, Phone: (312) 413 9683, FAX: (312) 996 6044, e-mail: tomdkw@uic.edu, Web: http://dentistry.uic.edu/CraniofacialGenetics, Oral Biol: http://dentistry.uic.edu/Depts/oralb/welcome.htm.

tissue is primarily due to the transdifferentiation of already committed cells or whether less differentiated cells within a given tissue are cued into commitment.

One of the multipotent tissues in the human body that has been attributed “progenitor” status (2–5) is the dental follicle, a seemingly homogeneous layer of ectomesenchymal cells surrounding the tooth germ outside of the outer dental epithelium and dental papilla in early stages of tooth bud formation (6,7). The dental follicle (dental sac) has long been considered the tissue of origin for periodontal ligament, root cementum, and alveolar bone (8–10). Most recently, we have proposed that the role HERS is to maintain the non-mineralized status and spatial architecture of the mammalian periodontal ligament (11–12).

There have been a number of studies that have suggested the presence of progenitor cells in the dental follicle (2,3,5,13,14). Under defined culture conditions, these fibroblastoid dental follicle progenitor cells were capable of differentiating into cementoblast/osteoblast-like cells (5,14–16). The differentiation potential of dental follicle cells has been confirmed during *in vivo* experiments (2,3,15,17). However, when implanted into immunodificient mice, dental follicle cells formed ligament-like fibrous and cementum-like mineralized tissue (2,3), suggesting that the dental follicle may either contain heterogeneous populations of progenitor cells, or that the progenitor cells possess multilineage differentiation potential.

Here, we have performed a series of experiments in order to further explore the question whether the seemingly homogeneous mesenchymal dental follicle contains heterogeneous cell populations. First, we have used histochemical and immunohistochemical assays to identify distinct cell types reflecting its pluripotent developmental potential. We have then generated three immortalized cell lines from dental follicle preparations which were vastly different in terms of cell shape, alkaline phosphatase activity, mineralization pattern, and gene expression pattern, and which were also distinctly different from a same-stage alveolar bone-derived cell line. Our findings indicate that the dental follicle contains at least three unique and distinct cell populations and that some of them could be used to regenerate periodontal tissues.

Materials and Methods

Tissue preparation for histology

For histochemical and immuhistochemical analysis, eight days postnatal Swiss Webster mice were sacrificed according to UIC Animal Care guidelines and mandibles prepared for fixation in 10% buffered formalin. Fixed tissues were prepared for frozen sections, paraffin sections, and ground sections. Our techniques for immunohistochemistry have been described previously (10,18).

Isolation of dental follicle cells

Dental follicle tissues from mouse molar developing tooth organs of eight days postnatal Swiss Webster mice (Charles River Laboratories, Wilmington, MA) were dissected. Dental follicles form a compact connective tissue unit that can easily be separated from surrounded tissues via careful dissection. Follicle tissues were then digested in a 5mg/ml collagenase/dispase solution (Roche Applied Science, Indianapolis, IN) with rotation at 37°C for 30 min. Primary cells were plated in 6-well plates containing Minimum Essential Medium Alpha Medium (α-MEM) supplemented with 10% FCS and 100 units/ml of penicillin/streptomycin. The plastic adherent cells were cultured until sub-confluence and then expanded into 100mm dishes.

Differentiation induction of primary dental follicle cells

Primary dental follicle (DF) cells were induced to differentiate into adipogenic, chondrogenic, and osteogenic lineages using various induction mediums (Cambrex, Walkersville, MD). For

adipogenic differentiation, 2×10^5 cells were plated into each well of a 6-well plate. At 100% confluence, three cycles of induction/maintenance were used to stimulate optimal adipogenic differentiation according to the manufacturer's instruction (Cambrex). Each cycle consisted of feeding the DF cells with adipogenic induction medium for 3 days followed by 3 days of culture in adipogenic maintenance medium. The presence of mature adipocytes was assessed by Oil Red O staining of cultures. For chondrogenic differentiation, cells were concentrated to a number of 2.5×10^5 per pellet to form chondrogenic pellets. The cell pellets were cultured in 15 ml polypropylene culture tubes and fed every 3 days with chondrogenic induction medium. Pellets were then harvested after 21 days in culture, formalin fixed and paraffin embedded. 5-μm sections were cut and stained with H & E or Alcian Blue to detect glycosaminoglycans using routine laboratory protocols. For osteogenic differentiation, 2×10^6 cells were seeded in 50 μl of PEGDA solution (Poly[ethylene glycol]diacrylate, MW 3400; Shearwater Polymers, Huntsville, AL) containing a photoinitiator (2-hydroxy-1-[4-(hydroxyethoxy)phenyl]-2-methyl-1-propanone; Ciba, Tarrytown, NY) at a final initiator concentration of 0.05% w/v. The cell/polymer suspension was photopolymerized at a wavelength of 365 nm and intensity of 4 mW/cm^2 using a long-wave ultraviolet lamp (UVP, Upland, CA). The cell-hydrogel constructs were cultured in osteogenesis induction medium (Cambrex) for 21 days, fixed in formalin and embedded in paraffin. The formation of mineralized nodules was detected with von Kossa staining.

Immortalization of DF cell lines

3×10^5 cells/well of DF cells were seeded into 6-well plates and cultured for 24 hrs. The cells were then transfected with 4μg of pSV3 plasmid DNA (ATCC, Manassas, VA) containing SV40 T large antigen, 8μl of PLUS reagent and 6ul of LipofectinAmine (Invitrogen, Carlsbad, CA) for 3 hrs. After removal of the DNA-PLUS-LipofectAMINE complex, cells were incubated in 2ml of complemented medium for three days. The cultures were changed to selection medium (α-MEM with 10% FCS, 250 μg/ml of G418) and grown for one month. Visible cell colonies were collected by using sterile Whatman paper soaked in 0.25% trypsin and serially diluted in 96-well plates. Single cells were expanded into cell lines.

Flow cytometry for cell phenotype and cell cycle analysis

For phenotypic characterization of cell lines, cells were cultured for 48 hrs and then harvested in 0.25% trypsin/EDTA. 10^6 cells were stained with FITC-conjugated anti-mouse CD13 (BD Biosciences, San Diego, CA), CD29, CD44 (BioLegend, San Diego, CA), CD90 (Cedarlane, Ontario, Canada) or PE-conjugated CD34 (RDI Research Diagnostics, Inc., Flanders, NJ) in 100μl of Dulbecco's PBS containing 2.5% BSA and 0.1% sodium azide for 45 min on ice according to the manufacturer's instructions. For non-conjugated anti-mouse CD105 (R&D Systems, Inc.,) and CD117 (RDI Research Diagnostics, Inc) antibodies, the cells were incubated with each first antibody for 45 min, and then stained with secondary mouse anti-rat IgG-FITC (Jackson ImmunoResearch, West Grove, PA) for another 45 min. Isotype controls were run in parallel using the same concentration of each antibody tested. For cell cycle analysis, 10^6 cells were trypsinized and pelleted by centrifugation. The cells were then fixed in 70% ethanol at 4°C for 1 hr, digested with 10ug/ml RNase A at room temperature for 30 min and stained with 10mg/ml propidium iodide (PI) for 30 min. The labeled cells were analyzed by flow cytometry in UIC Research Resources Center.

MTT cell proliferation assay

DF cells were seeded into 96-well plates at a density of 1×10^4 cells. The cells were then incubated for 24, 48 and 72 hrs, after which MTT (tetrazolium salt 3-(4,5-dimethylthiazol-2-yl)-2,5-diphenyl tetrazolium bromide) assay stock solution was added to a final concentration of 0.5mg/ml. To control for background absorbance, eight wells of cells were lysed by the

addition of Triton X-100 to a final concentration of 0.1% v/v immediately prior to the addition of MTT reagent. After incubation for 3hrs, the insoluble product was dissolved by addition of 100μl of cell lysis buffer (20% w/v SDS, 50% v/v dimethylformamide, pH 4.7), and absorbance of the wells was measured at 570 nm using a DU Series 60 Spectrophotometer (Beckman, fullerton, CA).

Alkaline phosphatase activity and von Kossa Staining

For alkaline phosphatase activity determination, 5×10^4 cells/well were seeded in 6-well plates and cultured until confluence. The cultured cells were washed with phosphate-buffered saline (PBS), incubated with NBT/BCIP staining solution for 15 min and then fixed in 8% paraformaldehyde. A similar procedure was applied to determine alkaline phosphatase activity on frozen sections. For von Kossa staining, 5×10^4 cells/well were seeded in 6-well plates. After confluence, the cells were incubated with 50μg/ml of ascorbic acid and 5 mM β-glycerophosphate in α-MEM medium containing 10% FCS for 2 weeks. The cells were treated with 5% silver nitrate solution as previously described (19). This procedure was applied to ground sections to determine mineralization behavior in eight days postnatal periodontal tissues.

Semi-quantitative RT-PCR

Total RNA was extracted from DF cells using TRIZOL LS Reagent (Invitrogen). Quality and quantity of the RNA was tested with spectrophotometry and agarose gel electrophoresis. 2μg of the RNAs were reverse transcribed and the cDNA was amplified using selected primers (Table 1) and the polymerase chain reaction (PCR) technique. RT-PCR products were then confirmed by sequencing analysis and run through agarose gel electrophoresis with a β-actin internal control and a DNA ladder.

Real time quantitative PCR

Real time quantitative PCR was conducted using SuperScript III Platinum two step qPcr kit with LUX fluorogenic primer (Invitrogen). Primer sequences for FGF9, BMP4, Runx2 and Col I genes are shown in table 1, and designed by LUX™ Designer (FAM labeled LUX primer Invitrogen). Reaction conditions were as follows: 2min at 50°C (one cycle). 10 min at 95°C (one cycle), and 15 second at 95°C and 1 min at 60°C (40 cycle). PCR products were continuously monitored with an ABI PRISM 7900 detection system (RRC-Core at UIC). Samples were normalized using ribosome 18 RNA (JOE labeled LUX primer set, Invitrogen). Results are expressed as hold increases of stimulation over control group by using the $2^{-\Delta\Delta Ct}$ method (20).

Immunohistochemistry

In order to determine levels of fibronectin expression, immunoreactions were performed as previously described (18,21). Affinity purified anti-human fibronection was used as primary antibody (Sigma, St Lois, MI). In previous studies, this antibody cross-reacted in mice in a tissue-specific fashion (data not shown). Anti-rabbit IgG was applied as a secondary antibody. For BrdU labeling, mouse anti-BrdU antibody (Zymed, South San Francisco, CA) was used as a detection system. Signals were detected using AEC as a substrate. In between these steps, slides were washed in phosphate buffered saline. The following controls were used to determine the specificity of the anti-fibronectin antibodies: (i) tissue controls - the specificity of the antibody will be evaluated in tissues with known immunoreactivity (ii) antibody controls by using a dilution series, (iii) controls with preadsorbed antibody to exclude unspecific binding, (iv) controls with pre-immune serum to control for binding to serum components and (v) omission of primary antibody as a systemic control.

Western blotting

Cells were lysed directly after washing in PBS with SDS-PAGE sample buffer. Same amount of the protein extracts from all four cell lines were separated on a 10% SDS-PAGE gel and transferred to nitrocellulose in a blotting apparatus filled with transfer buffer (25mM Tris, 190 mM glycine, 20% methanol) for 1 hour at 75 mA. Nitrocellulose filters were blocked in 2% BSA overnight at room temperature. The blot was incubated with 1:1000 dilution of anti-human cyclin D1 antibody (Santa Cruz, Santa Cruz, CA) for 2h, with 1:2000 dilution of AP-conjugated rabbit anti-goat secondary antibody (Zymed, South San Francisco, CA) for 1h, and then with NB/BCIP substrate. Controls omitting the primary antibody were all negative.

Statistical analysis

Student's t test was used for statistical analysis and $p < 0.05$ was taken as significant.

Results

Histochemical and immunohistochemical characterization of heterogenous cell populations in the dental follicle in situ

Our overview histochemical analysis identified the dental follicle as a loose connective tissue structure surrounding the developing tooth organ (Fig. 1). Further analysis via BrdU staining revealed numerous S-phase nuclei in the dental follicle and periodontal ligament (Fig. 1). Alkaline phosphatase activity was high in all three tissues, dental follicle, periodontal ligament, and alveolar bone, with intense reaction products in the immediate periphery of the mineralizing alveolar bone (Fig. 1). There was also high alkaline phosphatase activity in the stratum intermedium. Inorganic phosphates in the mineralized tissues alveolar bone and root dentin were labeled intensely via von Kossa's stain (Fig. 1). In addition, there were granular silver precipitates in the periodontal ligament, as well as intensely labeled nodules in the dental follicle, indicative of calcium phosphate mineral (Fig. 1). Fibronectin immunolabeling was intense in the differentiated periodontal ligament and in the dense coronal portion of the dental follicle, while fibronectin was not detected in other portions of the dental follicle (Fig. 1). In addition, immunoreactions for fibronectin were especially strong in the stellate reticulum (Fig. 1). Control stainings for fibronectin were negative.

Dental follicle primary cell lines formed colonies and displayed chondrogenic, adipogenic, and osteogenic phenotypes following differentiation induction

In order to examine colony-forming and multipotential differentiation capacities of dental follicle cells, primary dental follicle cell cultures were subjected to a variety of treatment modes. DF cell cultures formed colonies from single progenitor cells (Fig. 2A) and displayed multipotential characteristics following fate-specific induction (Fig. 2B–F). Specifically, (i) oil red-positive lipid-vacuoles were generated using adipogenic induction and maintenance strategies (Fig. 2B), (ii) a glycosaminoglycan-rich fibrous cartilage-type extracellular matrix following chondrogenic induction was revealed using alcian blue staining (Figs. 2C and D), and (iii) von Kossa positive reaction for inorganic phosphate minerals indicative of mineralized tissue formation was detected following osteogenic induction (Figs. 2E and F).

Immortalized dental follicle cell lines were positive for mesenchymal stem cells markers and did not express ameloblasts/odontoblast-related genes

The dental follicle and alveolar bone cell populations were seeded into 6-well plates and expanded into 100 mm dishes. At the third passage, the primary cultures were transfected with pSV-3 vector containing SV40 T-antigen to immortalize the cells. After G418 selection, more than 50 cell colonies were isolated and generated into cell lines. Three cell lines (DF1, DF2 and DF3) from the cell population of dental follicle, and one (AB1) from the alveolar bone cell

population were choose for further studies. Immortalization of the cells was confirmed by RT-PCR analysis of T-antigen expression. SV40 T antigen was detected in DF1, DF2, DF3 and AB1 cells, but not in the parental cells (Fig. 3A). All four cell lines expressed neither amelogenin nor dentin sialophosphoprotein genes (Fig. 3B), which were used as specific markers for ameloblasts and odontoblasts, respectively. These cell lines maintained growth over 30 passages.

The four immortalized cell lines demonstrated varying morphologies. DF1 featured typical elongated fibroblastic cell shape. DF2 cells were spindle-shaped with long processes. DF3 and AB1 cells were polygonal (Fig. 3C). Cell surface antigen profiles obtained by flow cytometry revealed that all four cell lines were negative for CD34 and CD117, and positive for CD44, CD29 and CD105. CD13 profiles were slightly positive for DF2 cells (Fig. 3D).

Mouse dental follicle cell lines were distinct in terms of proliferation rates and cell cycle distribution patterns

To evaluate cell growth rates of different DF cell lines, MTT cell proliferation assays were conducted. DF1, DF2, DF3 and AB1 cells were cultured in 96-well plates for 24, 48 and 72 hrs. At the end of the culture period, MTT was added for 4 hrs. The amount of color produced was measured at 570 nm. Data are presented here as mean absorbance +/− STD, which is directly proportional to the number of viable cells in each sample. The growth curves of these cells at passage 6–8 are shown in Fig. 2A, and display higher growth rates in DF1 and DF2 cells compared to lower growth rate in DF3 and AB1 cells at all three time points. The distribution of DF1, DF2, DF3 and AB1 cells during the cell cycle was examined by flow cytometry of propidium iodide-stained cells. G1 phase cell cycle distribution percentages were 37.2, 37.4, 43.5 and 50.6, for DF1, DF2, DF3 and AB1 cells, respectively (Fig. 4B). Cell cycle distribution patterns were further analyzed by cyclin D1 expression studies. Western blot analysis revealed highest cyclin D1 expression levels in DF2 cells, followed by DF1, DF3 and AB1 cells (Fig. 4C).

Dental follicle cell lines demonstrated significant differences in terms of mineralization potential

To determine the potential of DF cell lines to differentiate into mineralized tissue, DF1, DF2, DF3 and AB1 cells were analyzed for alkaline phosphatase activity and for mineralized nodule formation. There was extremely strong alkaline phosphotase reactivity in the DF1-line, followed by slightly reduced reactivity levels in DF3 and AB1 cells, and only weak alkaline phosphatase activity in DF1 cells (Fig. 5A). Von Kossa reactions showed little or no phosphate precipitation in DF2 cells, while there were strong reaction products in AB1 and DF3 cells. Spots of intense mineralization surrounding cell membranes alternated with little or no mineralization products in DF1 cell cultures (Fig. 5B). Hot RT-PCR analysis using primers for osteocalcin, an osteoblast/cementoblast marker gene, demonstrated that the osteocalcin gene expression was extremely strong in the dental follicle cell line DF3 as well as the alveolar bone cell line AB1. DF1 reaction was less and DF2 reaction was the weakest (Fig. 5C).

Differences in growth factor and matrix proteins gene expression patterns between distinct dental follicle cell lines

Cell differentiation is a dynamic process which involves sequential function cascades of growth factors, transcription factors and extracellular matrix proteins (22). Here we examined gene expression patterns in order to explore the differentiation stage of dental follicle cell lines. Real time RT-PCR analysis revealed distinct patterns of Fgf9 and BMP4 gene expression in DF1, DF2, DF3 and AB1 cells. Both Fgf9 and BMP4 were strongly expressed in DF1 cells. DF2 cells showed gene expression at a lower level compared to DF1 cells. Only basic expression levels of Fgf9 and BMP4 were observed in DF3 and AB1 cells (Fig. 6A). The expression of

CBFa1 type III was demonstrated to be expressed in all DF cell lines, showing slightly higher expression in DF2 and DF1 cells and lower expression in DF3 cells as compared to AB1 cells (Fig. 6A). Real time RT-PCR analysis revealed a similar expression level for Col I in AB1 and DF1 cells, while Col I expression was 43% lower in DF3 cells and 88% lower in DF2 cells when compared with AB1 cells (Fig. 6A).

The expression of a number of other extracellular matrix proteins was also evaluated. The level of tropoelastin mRNA expression was higher in DF1 and DF2 cells and very low in DF3. There was no detectable expression of tropoelastin in AB1 cells (Fig. 6B). The expression of both osteopontin and osteonectin was positively detected with no difference in all DF cell lines by RT-PCR analysis (Fig. 6). Immunoreactions for fibronectin demonstrated positive reactivity in all four cell lines, with strongest reactivity for DF2, followed by AB1 and DF1 (Fig. 6C). Controls were negative.

Discussion

Here we have established three heterogeneous dental follicle cell lines and compared these among each other and with a same-stage alveolar bone-derived cell line in terms of morphology, proliferation state, mineralization characteristics, and gene expression. Establishment of these distinct cell lines suggested the presence of a heterogeneous cell population in the developing dental follicle, possibly related to the different terminal differentiation states of follicle development, cementoblasts, alveolar bone osteoblasts, and periodontal ligament fibroblasts, and might also include a lineage-uncommitted pluripotent stem cell line (DF2). While no direct correlation between target tissues and cell lines was established, our data nevertheless suggested the presence of highly distinct cell populations with vastly different cellular characteristics in a light microscopically homogeneous mesenchymal tissue, the dental follicle.

While the dental follicle appeared as a fairly uniform fibrous tissue layer in response to simple histological stains on tissue sections, further histochemical, cytological and immunohistochemical assays in this paper established the presence of heterogenous cell populations in regions in which the dental follicle differentiated into its target tissues periodontal ligament and alveolar bone. Specifically, the undifferentiated dental follicle featured high proliferation activity, isolated mineral nodules, and high fibronectin levels in the dense coronal portion of the follicle. Regions of the dental follicle that were differentiating into periodontal ligament derivatives were high in fibronectin and contained low levels of mineral precipitates. In contrast, alveolar bone as a dental follicle derivative featured comparatively lower levels of fibronectin, dense mineral deposits, and an intense alkaline phosphatase lining in the periostal region. Together, these findings suggest that the dental follicle contains heterogenous cell populations, in part reflective of their terminal differentiation state such as alveolar bone or periodontal ligament. Our studies also established a possible link with classic embryological studies distinguishing between an inner layer of the dental follicle possibly related to cementogenesis, an intermediate layer related to the periodontal ligament, and an outer layer related to alveolar bone (23,24). Yet, the assays used in this study did not provide any evidence to establish a three-layer identity of dental follicle components based on histochemical and immunohistochemical analyses alone. Consequentially, the question remains unresolved whether alveolar bone, cementum, and periodontal ligament arise from a heterogeneous dental follicle cell population that differentiates at the target sites based on local signals or whether the dental follicle is a structure compartmentalized into discrete layers that are pre-determined to secrete tissue-specific extracellular matrices prior to completion of their homing process.

Our assays revealed distinct differences between the three dental follicle-derived cell lines in terms of proliferation rates, cell cycle distribution patterns, and cell surface markers. The high proliferation potential of DF1 and DF2 cells as documented in our proliferation assays was further confirmed by a higher percentage of S, G2, and M-phase cells and greater expression of cyclin D1. In comparison, DF3 and AB1 cells demonstrated lower proliferative activity, as our related assays indicated, including proliferation and cell cycle assays. Therefore, these studies suggest significant differences between DF1 and DF2 dental follicle cells compared to DF3 and alveolar bone derived cell lines in terms of proliferative activity. The positive labeling results for the cell activation marker CD13 provided further evidence for a high proliferative capacity of DF2 cells were (25). In addition, all four lines were positive for mesenchymal stem cell (MSC)-related surface antigens, CD44, CD29 and CD105, indicating that those cells were mesenchymal cells and may differentiate from the same origin. Cell surface marker presentation was consistent in that all four cell lines (DF1, DF2, DF3 and AB1) were negative for markers of hematopoietic lineage, CD34 and CD117.

All four cell lines generated in this study were remarkably different in terms of mineralization characteristics *in vitro*. The DF3 and AB1 cell lines displayed typical characteristics of mineralizing cell lineages as documented by their alkaline phosphatase activity and von Kossa stain. Both lines also expressed high levels of a typical biomineralization marker, osteocalcin, confirming our speculation that DF3 and AB1 cell lines may be typical differentiated osteoblast/cementoblast-like cells. DF1 and DF2 cell lines were significantly different from the DF3 and AB1 cell lines in their biomineralization characteristics. DF1 and DF2 only induced negligible levels of inorganic phosphate precipitates using von Kossa's stain and both of them expressed low levels of osteocalcin, indicating a lack of involvement in biomineralization events. Alkaline phosphatase activity was clearly higher in DF3 and AB1 cells compare to DF1, lending further support to our argument that DF3 and AB1 might be of osteoblast/cementoblast lineage, and DF1 might not be involved in mineralization. Osteocalcin gene expression and von Kossa staining are classic indicators for osteogenic differentiation in cell culture (15,26). In terms of alkaline phosphatase activity, data interpretation is less straightforward since it may be indicative both of mineralization events (27) and/or a low differentiation state of cells (28). At this low level of biomineralization activity, the high level of alkaline phosphatase activity in DF2 is more likely to reflect its undifferentiated state (28) than any potential involvement in biomineralization. Similarly, the differences in alkaline phosphatase activity between DF3 and AB1 considering the otherwise almost identical mineralization behavior might once more be reflective of a less differentiated state of DF3 compared to AB1. Together, our studies using osteocalcin, von Kossa, and alkaline phosphatase assays revealed DF3 and AB1 as mineralizing cementoblast/osteoblast lineages, while DF1 and DF2 may be classified as non-mineralizing progenitor cells (DF1) or pluripotent undifferentiated cells (DF2).

One of the unexpected findings of this study were the presence of von Kossa-positive inorganic phosphate mineral precipitates in the periodontal ligament as well as the occurrence of circumscribed mineralization events in the intercellular space of dental follicle islands. *In vitro*, the circumscribed mineralization events in the dental follicle were echoed in isolated mineralization islands surrounding cultured DF1 cells. While the differences between the mineralizing matrix islands of the dental follicle and the granular mineral deposits in the periodontal ligament are difficult to interpret at this point, we argue that the more general finding of biomineralization events in the periodontal soft tissues dental follicle and periodontal ligament is in congruence with our earlier theories of a fundamentally mineralizing nature of the vertebrate periodontium as an evolutionary basal feature to facilitate tooth attachment via ankylosis (11,12). According our findings, the non-mineralized status of the mature periodontal ligament is rather a result of mineralization inhibition control via HERS as a secondary event than a primary lack of mineralization capabilities (11,12).

Our results indicated that there were significant differences in growth factor and matrix proteins gene expression patterns between distinct dental follicle cell lines. Specifically, levels of BMP4 and Fgf9 expression were highest in DF1 cells, followed by DF2 cells. DF3 and AB1 cells displayed only basal levels of BMP4 and Fgf9 expression. Fgfs and BMPs are growth factors known to play important roles during tooth development (29,30). In situ hybridization and immunohistochemistry analysis demonstrated that both FGFs and BMPs were expressed in dental follicle cells involved in root- and ligament-forming stages (31,32). The expression levels of these growth factors were significantly downregulated in further differentiated tissues (33). FGFs and BMPs frequently display synergistic effects in development and osteogenetic differentiation *in vitro* and *in vivo* (29,34,35). One example is the ability of FGFs to facilitate BMP2-induced osteogenesis by altering the expression of endogenous BMPs or BMPRs on the surface of bone forming progenitor cells (34,35). The concept of a synergism between FGFs and BMPs related to osteogenic lineage differentiation is supported here by a synchronicity of expression levels, with highest levels in the undifferentiated cell line DF1, followed by DF2, and relatively low levels of expression in the high levels of mineral producing cells lines DF3 and AB1. All cell lines expressed CBFa1/Runx2, the earliest differentiation marker for committed osteogenetic precursor cells (35), indicative of their commitment toward an osteoblastic/cementoblastic lineage.

There have been a number of studies in support of the suitability of the dental follicle for tissue regeneration based on its capability to differentiate into cementum, periodontal ligament and alveolar bone following stimulation with growth factors and extracellular matrix proteins (33,36). As discussed above, the dental follicle's capacity to regenerate is probably not due to stem cells but rather an accomplishment of progenitors that may either be induced to commit to certain lineages or stimulated to pursue already pre-committed pathways in heterogenous cell populations. Heterogeneous populations as well as multilineage differentiation potential of dental follicle cells raise the possibility that dental follicle cells may differentiate into different or undesired lineages when used for periodontal regeneration. Previous studies have revealed that dental follicle cells without induction of differentiation fail to mineralize or form both ligament-like fibrous and cementum-like mineralized tissue *in vivo* (2,3,17). Therefore, directing the differentiation of stem cells and progenitors into desired cell lineages *in vitro* might be a promising strategy for tissue repair and tissue regeneration (37). Application of this research toward the regeneration of human periodontal tissues would hold great promise for periodontal therapies.

References

1. Young HE, Black AC. Adult Stem Cells. Anat Rec 2004;276A:75–102.
2. Handa K, Saito M, Tsunoda A, Yamauchi M, Hattori S, Sato S, Toyoda M, Teranaka T, Narayanan AS. Progenitor cells from dental follicle are able to form cementum matrix in vivo. Connect Tissue Res 2002;43:406–8. [PubMed: 12489190]
3. Handa K, Saito M, Yamauchi M, Kiyono T, Sato S, Teranaka T, Narayanan AS. Cementum matrix formation in vivo by cultured dental follicle cells. Bone 2002;31:606–11. [PubMed: 12477575]
4. Saito M, Handa K, Kiyono T, Hattori S, Yokoi, Tsubakimoto T, Harada H, Noguchi T, Toyoda M, Sato S, Teranaka T. Immortalization of cementoblast progenitor cells with Bmi-1 and TERT. J Bone Miner Res 2005;20:50–7. [PubMed: 15619669]
5. Morsczeck C, Gotz W, Schierholz J, Zeilhofer F, Kuhn U, Mohl C, Sippel C, Hoffmann KH. Isolation of precursor cells (PCs) from human dental follicle of wisdom teeth. Matrix Biol 2005;24:155–65. [PubMed: 15890265]
6. Paynter KJ, Pudy G. A study of the structure, chemical nature, and development of cementum in the rat. Anat Rec 1958;131:233–51. [PubMed: 13583573]
7. Armitage GC. Periodontal diseases of children and adolescents. Cda J 1986;14:57–61. [PubMed: 3466717]

8. Schour, I., editor. Oral histology and embryology. Lea & Febiger; Philadelphia: 1960.
9. Diekwisch TG. The developmental biology of cementum. Int J Dev Biol 2001;45:695–706. [PubMed: 11669371]
10. Diekwisch TGH. Pathways and fate of migratory cells during late tooth organogenesis. Connect Tissue Res 2002;43:245–56. [PubMed: 12489167]
11. McIntosh JE, Anderton X, Flores-De-Jacoby L, Carlson DS, Shuler CF, Diekwisch TG. Caiman periodontium as an intermediate between basal vertebrate ankylosis-type attachment and mammalian "true" periodontium. Microsc Res Tech 2002;59:449–59. [PubMed: 12430171]
12. Luan X, Ito Y, Diekwisch TG. Evolution and development of Hertwig's epithelial root sheath. Dev Dyn. 2006
13. Luan X, Dangaria SJ, Diaz MZ, Yamane A, Diekwisch TGH. Human dental pulp and dental follicle stem cell differentiation. J Dent Res 2005;84:0035.
14. Morsczeck C, Moehl C, Gotz W, Heredia A, Schaffer TE, Eckstein N, Sippel C, Hoffmann KH. In vitro differentiation of human dental follicle cells with dexamethasone and insulin. Cell Biol Int 2005;29:567–75. [PubMed: 15951208]
15. Zhao M, Xiao G, Berry JE, Franceschi RT, Reddi A, Somerman MJ. Bone morphogenetic protein 2 induces dental follicle cells to differentiate toward a cementoblast/osteoblast phenotype. J Bone Miner Res 2002;17:1441–51. [PubMed: 12162498]
16. Hakki SS, Berr JE, Somerman MJ. The effect of enamel matrix protein derivative on follicle cells in vitro. J Periodontol 2001;72:679–87. [PubMed: 11394405]
17. Jin QM, Zhao M, Webb SA, Berry JE, Somerman MJ, Giannobile WV. Cementum engineering with three-dimensional polymer scaffolds. J Biomed Mater Res 2003;67:54–60.
18. Diekwisch TG, Ware J, Fincham AG, Zeichner-David M. Immunohistochemical similarities and differences between amelogenin and tuftelin gene products during tooth development. J Histochem Cytochem 1997;45:859–66. [PubMed: 9199671]
19. Diekwisch TG, Berman BJ, Gentner S, Slavkin HC. Initial enamel crystals are not spatially associated with mineralized dentine. Cell Tissue Res 1995;279:149–67. [PubMed: 7895256]
20. Livak KJ, Schmittgen TD. Analysis of relative gene expression data using real-time quantitative PCR and the 2-^^^{C}T method. Methods 2001;25:402–408. [PubMed: 11846609]
21. Thieberg RH, Yamauchi M, Satchell PG, Diekwisch TG. Sequential distribution of keratan sulphate and chondroitin sulphate epitopes during ameloblast differentiation. Histochem J 1999;31:573–8. [PubMed: 10579626]
22. Baksh D, Song L, Tuan RS. Adult mesenchymal stem cells: characterization, differentiation, and application in cell and gene therapy. J Cell Mol Med 2004;8:301–16. [PubMed: 15491506]
23. Ten Cate AR, Miis C, Solomon J. The development of the periodontium: A transplantation and autoradiographic study. Anat Rec 1971;170:365–380. [PubMed: 5088406]
24. Ten Cate AR. The development of the periodontium- a largely ectomesenchymally derived unit. Periodontal 2000 1997;13:9–19.
25. Rosenzwajg M, Tailleux L, Gluckman JC. CD13/N-aminopeptidase is involved in the development of dendritic cells and macrophages from cord blood CD34(+) cells. Blood 2000;95:453–60. [PubMed: 10627449]
26. Frank O, Heim M, Jakob M, Barbero A, Schafer D, Bendik I, Dick W, Heberer M, Martin I. Real-time quantitative RT-PCR analysis of human bone marrow stromal cells during osteogenic differentiation in vitro. J Cell Biochem 2002;85:737–46. [PubMed: 11968014]
27. Collin P, Nefussi JR, Wetterwald A, Nicolas V, Boy-Lefevre ML, Fleisch H, Forest N. Expression of collagen, osteocalcin, and bone alkaline phosphatase in a mineralizing rat osteoblastic cell culture. Calcif Tissue Int 1992;50:175–83. [PubMed: 1373988]
28. Sidhu KS, Tuch BE. Derivation of three clones from human embryonic stem cell lines by FACS sorting and their characterization. Stem Cells Dev 2006;15:61–9. [PubMed: 16522163]
29. Maas R, Bei M. The genetic control of early tooth development. Crit Rev Oral Biol Med 1997;8:4–39. [PubMed: 9063623]
30. Tucker AS, Yamada G, Grigoriou M, Pachnis V, Sharpe PT. Fgf-8 determines rostral-caudal polarity in the first branchial arch. Development 1999;126:51–61. [PubMed: 9834185]

31. Aberg T, Wozney J, Thesleff I. Expression patterns of bone morphogenetic proteins (Bmps) in the developing mouse tooth suggest roles in morphogenesis and cell differentiation. Dev Dyn 1997;210:383–96. [PubMed: 9415424]
32. Yamamoto T, Myokai F, Nishimura F, Ohira T, Shiomi N, Yamashiro K, Arai H, Murayama Y, Takashiba S. Gene profiling in human periodontal ligament fibroblasts by subtractive hybridization. J Dent Res 2003;82:641–5. [PubMed: 12885851]
33. Sena K, Morotome Y, Baba O, Terashima T, Takano Y, Ishikawa I. Gene expression of growth differentiation factors in the developing periodontium of rat molars. J Dent Res 2003;82:166–71. [PubMed: 12598543]
34. Nakamura Y, Tensho K, Nakaya H, Nawata M, Okabe T, Wakitani S. Low dose fibroblast growth factor-2 (FGF-2) enhances bone morphogenetic protein-2 (BMP-2)-induced ectopic bone formation in mice. Bone 2005;36:399–407. [PubMed: 15777655]
35. Fakhry A, Ratisoontorn C, Vedhachalam C, Salhab I, Koyama E, Leboy P, Pacifici M, Kirschner RE, Nah HD. Effects of FGF-2/-9 in calvarial bone cell cultures: differentiation stage-dependent mitogenic effect, inverse regulation of BMP-2 and noggin, and enhancement of osteogenic potential. Bone 2005;36:254–66. [PubMed: 15780951]
36. Hou LT, Liu CM, Chen YJ, Wong MY, Chen KC, Chen J, Thomas HF. Characterization of dental follicle cells in developing mouse molar. Arch Oral Biol 1999;44:759–70. [PubMed: 10471160]
37. Heng BC, Haider H, Sim EK, Cao T, Ng SC. Strategies for directing the differentiation of stem cells into the cardiomyogenic lineage in vitro. Cardiovasc Res 2004;62:34–42. [PubMed: 15023550]
38. Kölliker, A. Handbuch der Gewebelehre des Menschen. Vol. 5. Engelmann; Leipzig: 1867.

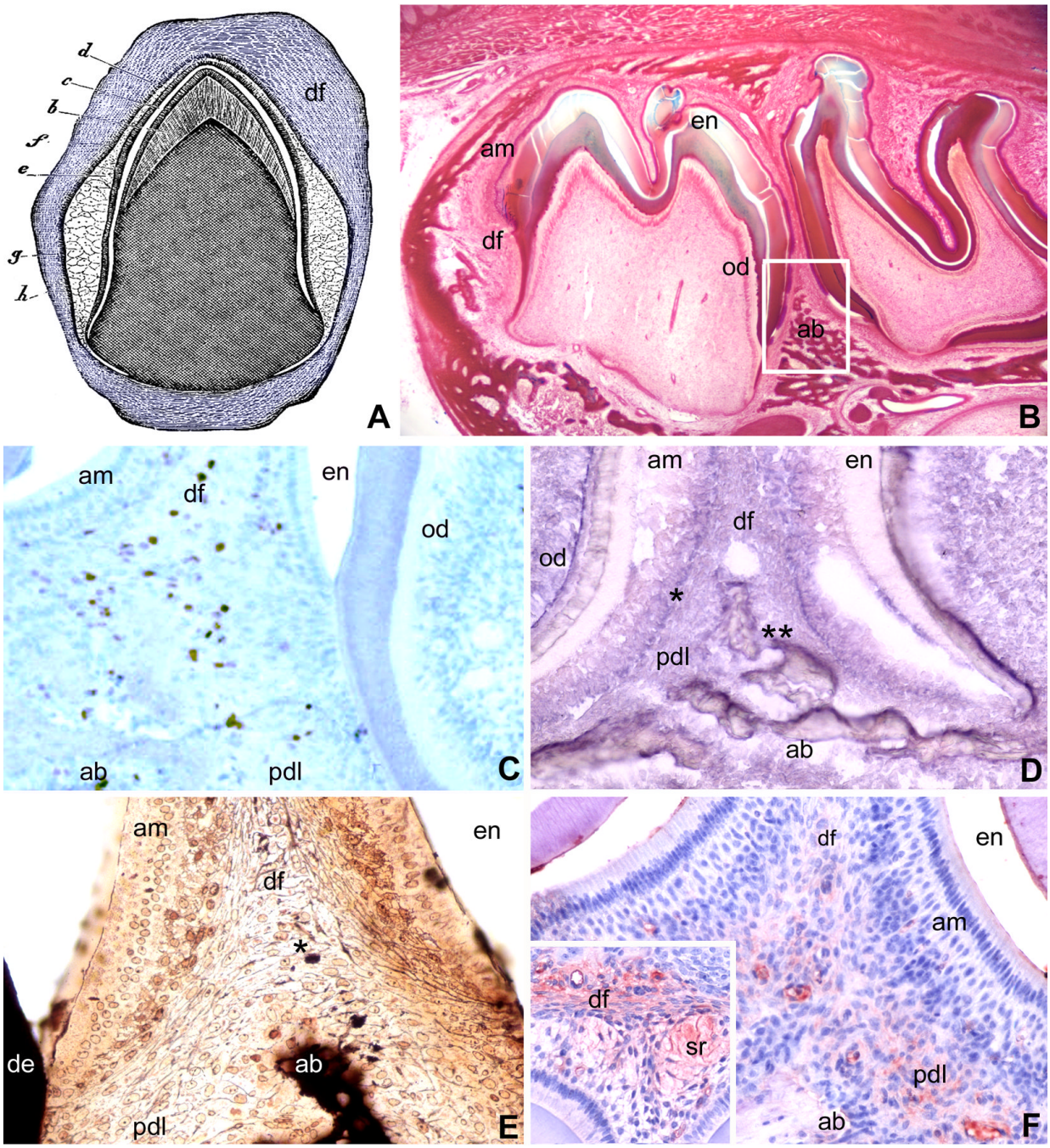

Fig. 1. Histochemical characterization of dental follicle

Fig. 1A is a historical drawing of a developing tooth organ from the famous 5th edition of Rudolph Albert von Kölliker's "Handbuch der Gewebelehre" (A Handbook of Human Microscopic Anatomy, Leipzig (38). The dental follicle (df) has been colorized in blue. In Kölliker's illustration, the follicle forms a seemingly homogeneous layer of connective tissue cells surrounding the developing tooth organ. Fig. 1B. This overview preparation of a developing mouse molar tooth organ reveals the dental follicle (df) as a loose connective tissue unit in the circumference of the developing tooth, surrounding ameloblasts (am), enamel (en), and odontoblasts (od). The area chosen for close-up micrographs in the subsequent four images is demarked by a rectangle and includes the tip of the developing alveolar bone (ab). Fig. 1C.

BrdU labeling of S-Phase nuclei in the dental follicle and periodontium of 12 days postnatal mouse molars. Proliferative activity in the dental follicle (df) and in the periodontal ligament (pdl) were higher than in the alveolar bone (ab). Fig. 1D. Alkaline phosphatase activity in the developing periodontium. There was no alkaline phosphatase in enamel (en), while all tissues of the developing periodontium contained alkaline phosphatase activity at this stage, including dental follicle (df), alveolar bone (ab), and periodontal ligament (pdl). Extremely high alkaline phosphatase activities were detected in the stratum intermedium (*) and the mineralizing alveolar bone margins (**). Figs. 1E and F. Detection of phosphate mineral deposits in the developing periodontium by von Kossa's procedure. Alveolar bone (ab) and root dentin (de) were heavily stained. Note the surprise detection of mineralizing nodules in the dental follicle (asterisk). There were also granular phosphate precipitates in the dental follicle (df) and in the periodontal ligament (pdl). Fig. 1G and H. Anti-fibronectin immunoreaction in the developing periodontium. In the inter-radicular region, there was a distinct staining for fibronectin in the periodontal ligament (pdl), while the reaction products in the dental follicle (df) and in the alveolar bone (ab) were less intense. Fig. 1H highlights the intense anti-fibronectin staining reactivity in the coronal portion of the dental follicle (df) and in the stellate reticulum (sr). For orientation purposes, ameloblasts (am) and enamel (en) were labeled in some micrographs.

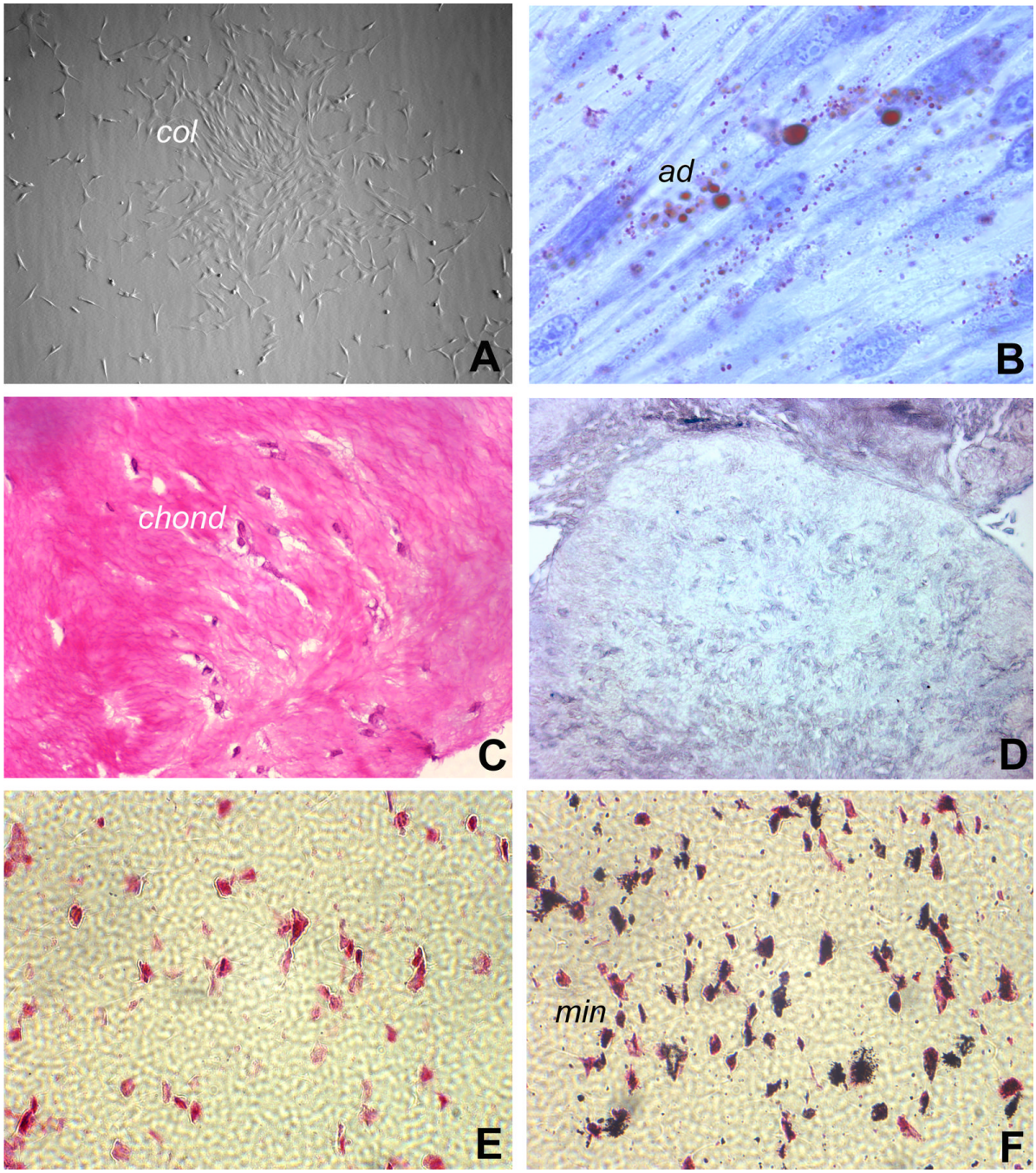

Fig. 2. Stem cell characteristics of dental follicle cells

In order to examine colony-forming and multipotential differentiation capacities of dental follicle cells, primary dental follicle cell cultures were subjected to a variety of treatment modes. A. Colony-forming efficiency of dental follicle cells. DF cells were planted into 150 mm culture dishes at a density of 10^4 cells/dish and cultured for 14 days. Fig. 2A represents a typical cell colony originated from a single progenitor cell. The morphology of the cells within the colony is fibroblast-like. B. Adipogenic differentiation potential of dental follicle cells. After three cycles of adipogenic induction/maintenance and 7 more days in maintenance medium, DF cells formed clusters of oil red-positive lipid vacuoles inside of the induced cells. Hematoxylin was used in this preparation to counterstain nuclei. Non-induced cells did not

contain any lipid vacuoles (data not shown). C and D, Chondrogenic differentiation potential of DF cells. DF cell pellets were cultured in chondrogenic induction medium for 21 days and then prepared for histological staining. C. H & E staining of paraffin sections of the pellets. The pellets contained spindle-shaped cells which were surrounded by a dense, fibrous extracellular matrix. D. Alcian blue staining of paraffin sections of induced pellets. The blue dye recognized the proteoglycan-rich extracellular matrix of the fibrous cartilage-type tissue in the induced pellet. E. Osteogenic differentiation potential of DF cells. DF cells were seeded in hydrogels and cultured in osteogenic induction medium for 14 days. Mineralized nodule formation was shown in von Kossa stained sections. The mineralization nodules were highly abundant in induced DF cells (E) and not present in non-induced control cells (F).

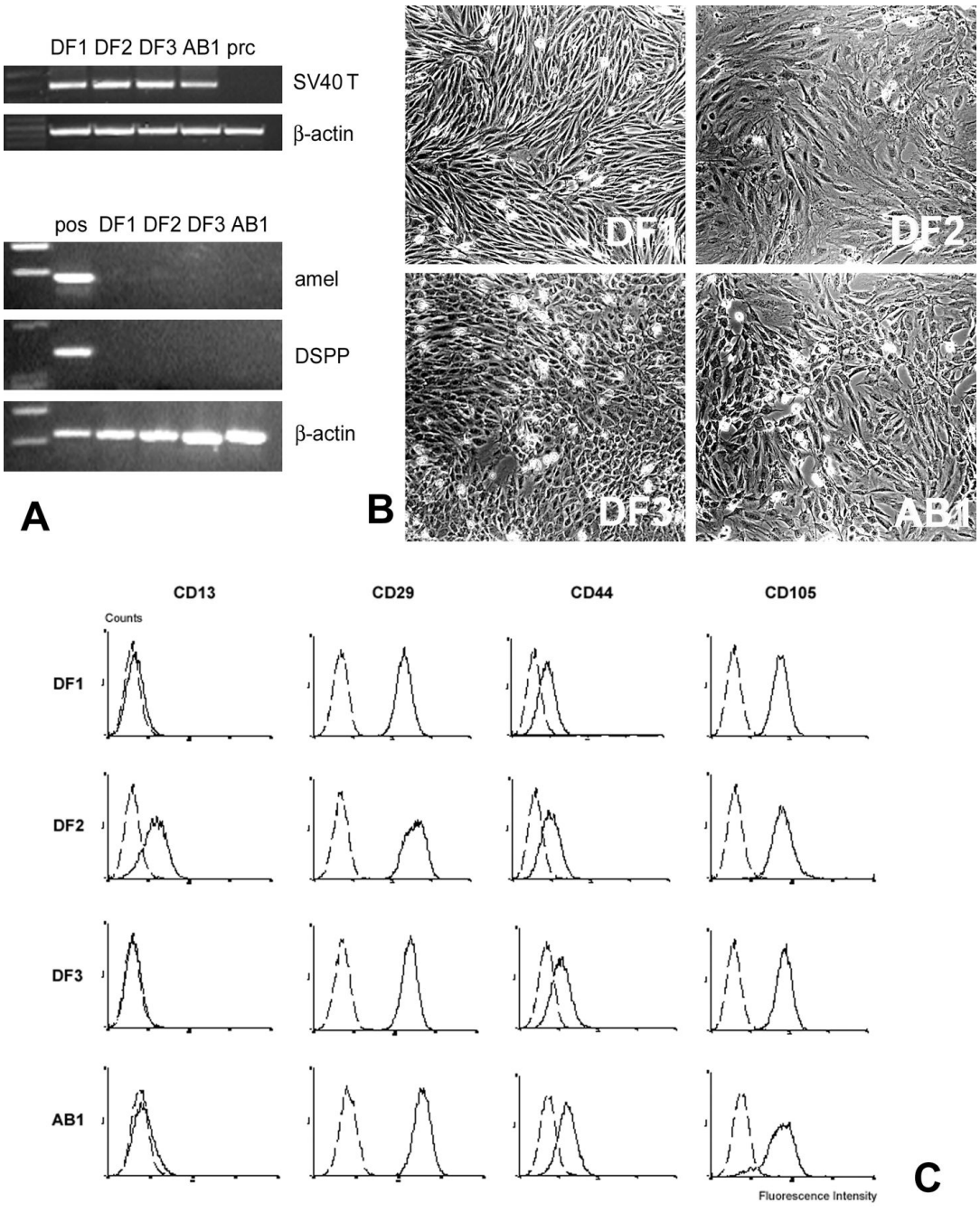

Fig. 3. Isolation and characterization of immortalized mouse dental follicle (DF) cell lines

In order to generate unique, dental follicle-derived cell lines, dental follicle preparations were phase-digested, converted into single cell suspensions, and seeded onto 6-well plates. Seeded dental follicle cells from preparation subgroups were transfected with the pSV3 vector containing the SV40 large T antigen and selected by G418. Four cell lines were selected for characterization. A. Expression of large T antigen was detected in all immortalized dental follicle cell lines by reverse transcription PCR using total RNA isolated from DF1, DF2, DF3 and AB1 cells, but not in the primary cells (prc). Expression of amelogenin and DSPP were not detected in DF1, DF2, DF3 and AB1 cell lines by RT-PCR analysis. Positive controls for amelogenin and DSPP genes are shown in the lane marked pos. B. Phase contrast micrographs

of DF cell lines. The DF1 cells were elongated and densely configured. DF2 cells were spindle-shaped and featured extremely long cell processes. The DF3 cell line contained densely packed polygonal cell shapes. The AB1 cell line was characterized by a transition between polygonal and spindle-shaped cell shapes. All four lines reveal distinct morphological phenotypes. C. Expression profiling of dental follicle cell lines for mesenchymal stem cell surface antigens using flow cytometry. The cell surface antibody used for characterization is indicated on the top of each column, the type of cell lines on the left side of each row. Labeled cells were analyzed using the WINMDI software (Purdue University, West Lafayette, IN). Dotted and solid lines in each histogram represent cells labeled with isotype-matched Ig and specific antibodies, respectively. All four cell lines were positive for CD29, CD44, and CD105, while only DF2 was also positive for CD13. DF1, DF3, and AB1 were negative for CD13. All four lines were negative for the hematological markers CD34 and CD117 (not shown).

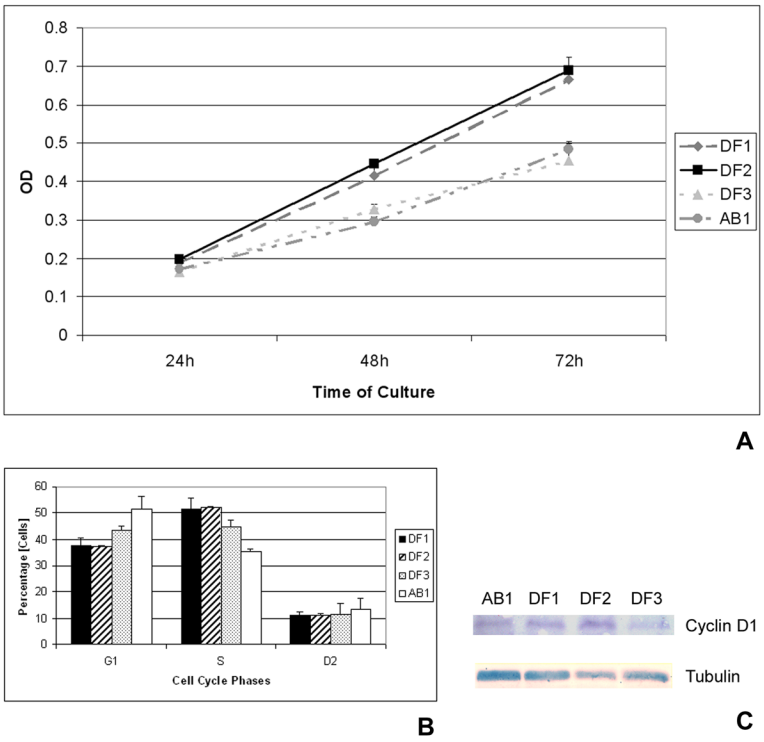

Fig. 4. Proliferation of mouse dental follicle cell lines

A. An MTT cell proliferation assay was conducted after DF1, DF2, DF3 and AB1 cells were cultured for 24, 48 and 72 hours. The amount of color produced was determined by measuring OD at 570 nm to assay proliferation of cultured cells. The data represent three experiments performed in triplicate. The MTT assay revealed 40% higher proliferation indices for DF2 and DF1 compared to DF3 and AB1. B. Assessment of cell cycle phases using Flow cytometry of propidium iodide-stained cells in DF1, DF2, DF3 and AB1 cell lines. Data represent the means ± standard deviation of three experiments. In comparison, DF1 and DF2 exhibited more cells in S-Phase than DF3 and AB1, while AB1 featured more cells in G1 phase than the other three lines. For DF3 cells, the ratio between G1-Phase and S-Phase cells was about even. C. Cyclin D1 detection in cell lysates of DF1, DF2, DF3 and AB1 cells after separation by SDS-PAGE and subsequent Western blotting. Following cyclin D1 recognition, membranes were re-probed to control for equal protein levels using anti-Tubulin antibody (lower panel). Note the strong labeling for cyclin D1 in DF2 cell lysates.

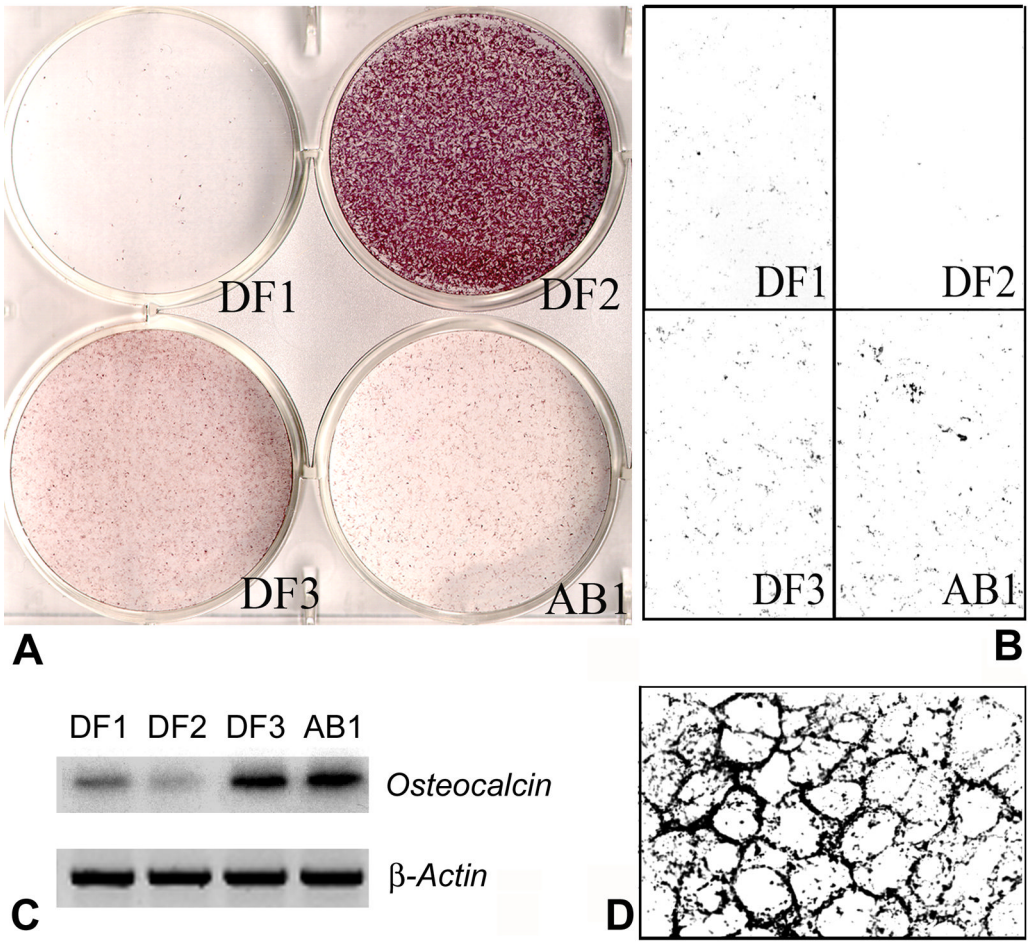

Fig. 5. Differentiation of dental follicle cells into mineralized tissues

DF1, DF2, DF3 and AB1 cells were plated at a concentration of 5×10^4/well in 6-well plates and cultured until confluence. For von Kossa staining and osteocalcin gene expression, cells were treated with ascorbic acid and β-glycerophosphate for 14 days. A. Alkaline phosphatase (ALP) activity was recorded after fixation and staining with NBT/BCIP staining solution. The ALP positive cells were identified by their purple staining. Note the extremely high alkaline phosphatase activity in DF2 cells, followed by low intensity alkaline phosphatase levels in DF3 and then AB1. DF1 was almost free of alkaline phosphatase activity. B. Mineralized nodule formation as revealed by von Kossa staining. C. Osteocalcin gene expression analysis via semiquantitative hot RT-PCR. Osteocalcin gene expression levels served as a marker for osteoblast/cementoblast differentiation. There was strong osteocalcin gene expression in the DF3 and AB1 cells compared to low level expression in DF1. DF2 cells were almost lacking osteocalcin expression.

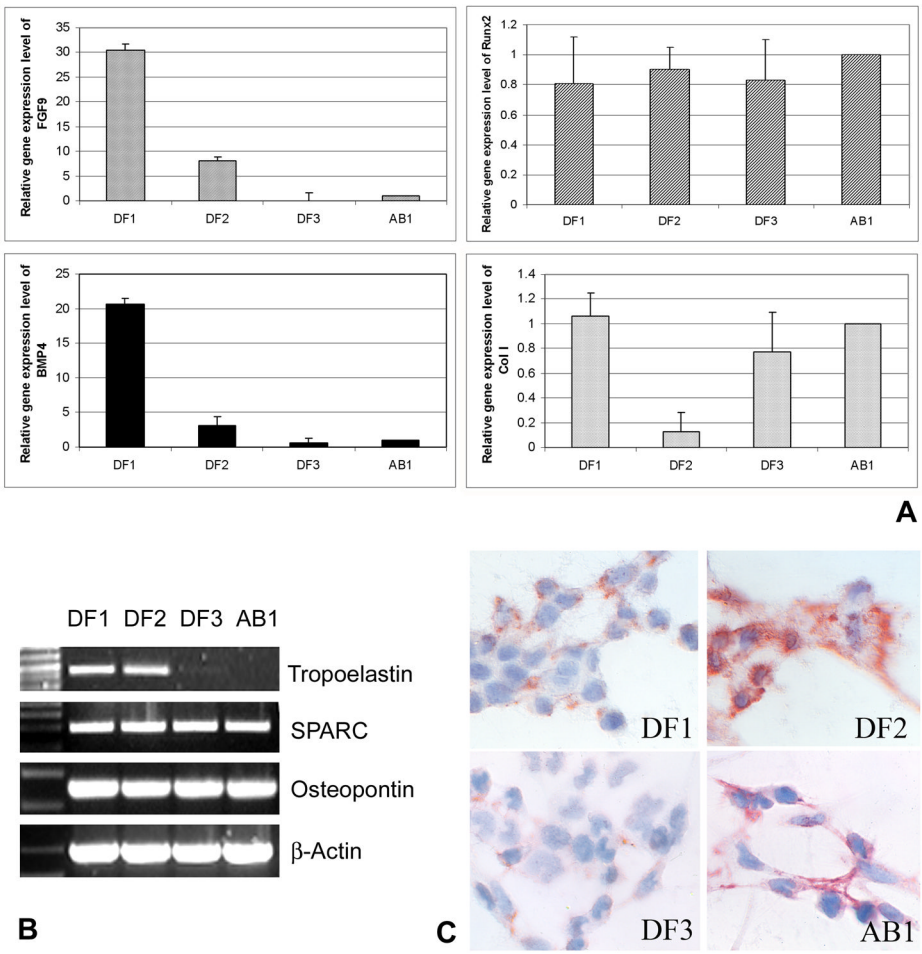

Fig. 6. Gene expression patterns of dental follicle cell lines

DF1, DF2, DF3 and AB1 cells were grown for 48 hours and reached sub-confluence. The cells were either extracted for isolation of total RNA, or fixed for immunohistochemistry analysis. A. Expression of growth factors Bmp4 and Fgf9, transcription factor CBFa1, and extracellular matrix protein Col I was determined by real time PCR analysis. B. Expression of extracellular matrix proteins osteopontin, osteonectin and tropoelastin was detected by RT-PCR analysis. C. Immunostaining patterns of DF1, DF2, DF3 and AB1 cells for fibronectin were demonstrated based on immunoperoxidase reactivity. The photograph showed ×40 magnification of the stained cells.

Table 1

Primers for RT-PCR amplification of growth factors, transcription factors, extracellular matrix genes, and house keeping genes used to characterized dental follicle derived and alveolar bone derived cell lines.

Gene	Orientation	Sequence
SV40 T antigen	S	GACTTTGGAGGCTTCTGGATGCAACTGAG
SV40 T antigen	AS	AGCAGACACTCTATGCCTGTGTGGAGTAAG
Amelogenin	S	AACCATCAAGAAATGGGG
Amelogenin	AS	TCGGTTCTCTCATTTTCTG
DSPP	S	ACGGGATAGAGGAGGATGA
DSPP	AS	TTCCACTGAGCCTTCCCAGA
Osteocalcin	S	CTTGCCTTCTGCCTGGGTGTCC
Osteocalcin	AS	GATGCGTTTGTAGGCGGTCTTCA
Osteopontin	S	GACCATGAGATTGGCAGTGATTTG
Osteopontin	AS	TGATGTTCCAGGCTGGCTTTG
Osteonectin (Sparc)	S	GTCCCACACTGAGCTGGC
Osteonectin (Sparc)	AS	AAGCACAGAGTCTGGGTGAGT
Tropoelastin	S	CTTGGTGGAGCCGGAGGATTG
Tropoelastin	AS	GGAGGGGGTGGTCATAGAAGGTTT
β-actin	S	GAGCAAGAGAGGTATCCTGAC
β-actin	AS	TTCATGGATGCCACAGGATTC
FGF 9	S	GACTCGTTCTTGTGCTTAAAAGCCGAGTC
FGF 9	AS	GCGTCCTGCACACCGAAATA
BMP 4	S	CACAGTAGCCGAGCCAACACTGTG
BMP 4	AS	TGGTCCCTGGGATGTTCTCC
Runx 2	S	CACAGGCGACAGTCCCAACTTCCTGG
Runx 2	AS	CTCTCCGAGGGCTACAACCTT
Type I Collagen	S	GAACCAGCCGATGATGCTAACGTGGTC
Type I Collagen	AS	GGCTGCGGATGTTCTCAATCT

Table 2

Cell Cycle Analysis of Dental Follicle Cell Lines

Note the high percentage of S-phase cells in the DF1 and DF2 lines indicative of high proliferation, the high percentage of G1-phase cells in the AB1 line representative of differentiated cells, and the DF3 line as an intermediary.

	DF1	DF2	DF3	AB1
G1	37.43+/−7.15	37.4+/− 0.2	43.50+/− 1.8	51.30+/− 4.98
S	51.33+/− 8.45	52.17+/− 0.35	44.93+/− 2.25	35.20+/− 0.90
G2	11.23+/−1.3	11.23+/− 0.5	11.57+/− 4.05	13.50+/− 4.10